ORIGINAL RESEARCH

The Value of TTPVI in Prediction of Microvascular Invasion in Hepatocellular Carcinoma

Tao Zhang[1],*
Gaurab Pandey[1],*
Lin Xu[1]
Wen Chen[1]
Liangrui Gu[1]
Yijun Wu[1]
Xiuwen Chen[2]

[1]Department of Radiology, Taihe Hospital, Hubei University of Medicine, Shiyan, Hubei, People's Republic of China; [2]Department of Pathology, Taihe Hospital, Hubei University of Medicine, Shiyan, Hubei, People's Republic of China

*These authors contributed equally to this work

Purpose: The objective of our study was to evaluate the value of two-trait predictor of venous invasion (TTPVI) in the prediction of pathological microvascular invasion (pMVI) in patients with hepatocellular carcinoma (HCC) from preoperative computed tomography (CT) and magnetic resonance (MR).

Methods: A total of 128 preoperative patients with findings of HCC were enrolled. Tumor size, tumor margins, tumor capsule, peritumoral enhancement, and TTPVI was assessed on preoperative CT and MRI images. Histopathological features were reviewed: pathological tumor size, tumor differentiation, pMVI along with alpha-fetoprotein level (AFP). Significant imaging findings and histopathological features were determined with univariate and multivariate logistic regression analysis.

Results: Univariate analysis revealed that tumor size ($p<0.01$), AFP level ($p=0.043$), tumor differentiation ($p<0.01$), peritumoral enhancement ($p=0.003$), pathological tumor size ($p<0.01$), tumor margins ($p<0.01$) on CT and MRI, and TTPVI ($p<0.01$) showed statistically significant associations with pMVI. In multivariate logistic regression analysis, tumor size (odds ratio [OR] = 1.294; 95% confidence interval [CI]: 1.155, 1.451; $p < 0.001$), tumor differentiation (odds ratio [OR] =1.384; 95% confidence interval [CI]: 1.224, 1.564; $p < 0.001$), and TTPVI (odds ratio [OR] = 4.802; 95% confidence interval [CI]: 1.037, 22.233; $p=0.045$) were significant independent predictors of pMVI. Using 5.8 as the threshold for size, one could obtain an area-under-curve (AUC) of 0.793, 95% confidence interval [CI]: 0.715 to 0.857.

Conclusion: Tumor size, tumor differentiation, and TTPVI depicted in preoperative CT and MRI had a statistically significant correlation with pMVI. Hence, TTPVI detected on CT and MRI may be predictive of pMVI in HCC cases.

Keywords: CT, MRI, hepatocellular carcinoma, microvascular invasion, two-trait predictor of venous invasion

Introduction

HCC is the sixth most common cancer and the most common primary malignant tumor of the liver, accounting for the second leading cause of death due to cancer in men worldwide.[1] Liver fibrosis is a hallmark of chronic liver disease (CLD), characterized by the excessive accumulation of extracellular matrix proteins. Untreated CLD leads to liver fibrosis, may progress to cirrhosis, which is the most critical risk factor for HCC.[2] However, the advent of newer imaging techniques and surveillance for risk stratification has led to early detection of HCC, resulting in the selection of patients with a value of curative resection.[3,4] Hepatic resection is a potential treatment modality for HCC.[5] But the high frequency of intra and extrahepatic recurrences have led to a poor prognosis.[6,7]

Correspondence: Lin Xu
Email linxu850@gmail.com

4097

Histopathologic features of vascular invasion (VI) by tumor is a poor prognostic factor for patients with HCC who have undergone hepatic resection or liver transplant. VI by tumor is a significant risk factor leading to the early recurrence of HCC.[8] In a study, Iwatsuki et al.[9] concluded that the risk of recurrence was 4.4-fold higher in pMVI, whereas 15-fold higher in macrovascular invasion for patients who had undergone liver transplantation for HCC, recurrence rates after hepatic resection can be as high as 50% within five years.[10] Preoperative diagnosis of involvement of pMVI is of utmost importance as it helps to predict the recurrence and prognosis in patients who have to undergo liver resection or transplantation. VI classified into two types: macrovascular invasion and microvascular invasion. Macrovascular invasion (tumor thrombus in the primary portal vein), which is easily detectable by various imaging procedures, is a relative contraindication for liver transplantation or resection.[11] Therefore, detection of pMVI before treatment helps determine treatment options and is an important parameter included in the various scoring systems.[12] Whereas, detection of pMVI is difficult even with the aid of sophisticated imaging techniques for patient evaluation before initiating the treatment for HCC. In recent days, many studies have reported for the association of pMVI with prognosis following liver transplantation or resection.[13–15] According to the Liver Cancer Study Group of Japan, large tumor size, multiple tumors, intrahepatic micrometastasis, poor histologic grade, and gross anatomic subtype are pathologic markers suggestive of an increased risk of pMVI.[16] pMVI includes the involvement of numerous microscopic vessels that are contiguous with the tumor leading to a wide range of outcomes even after tumor resection.[13] MVI is as crucial as macrovascular invasion and should evaluate in patients with HCC. In clinical practice, the presence of pMVI determined by using histologic assessment after resection, and preoperative prediction of MVI by using a noninvasive method remains difficult. Researches have tried to diagnose pMVI, including preoperative CT during hepatic angiography, dual-energy CT, dynamic MRI, Functional imaging (such as Diffusion-Weighted Imaging, Diffusion kurtosis imaging, Into-vexol Incoherent Movement), PET and radiomics.[17–24] These imaging techniques may help to predict the presence of pMVI. Imaging techniques including CT and MR which recommended for HCC diagnosis, are of great significance in clinical practice. Imaging features such as a TTPVI algorithm based on the association between imaging features and gene expression have previously suggested as reliable biomarkers of MVI.[25,26] However, these criteria for preoperative radiological diagnosis of microvascular invasion (rMVI) in HCC has not been widely recognized. TTPVI is rarely externally validated. Consequently, the purpose of our study was to explore the value of TTPVI in the prediction of pMVI in patients with HCC from preoperative CT and MRI.

Methods
Patients
This retrospective study was conducted between January 2016 and December 2018 with the approval from the institutional review board of Taihe hospital, affiliated to Hubei University of Medicine, Shiyan, and informed written consent obtained from all the 128 study participants. The enrollment of the patients was according to the following inclusion criteria: (1) Age ≥16 years; (2) Both sexes; (3) an HCC imaging diagnosis was reached according to the AASLD guidelines until 2010[27] and according to their updated versions until 2013;[12] (4) Time interval between preoperative CT, MRI study and surgery of less than one month; (5) No history of malignancy. Exclusion criteria were as follows: (1) HCC with macrovascular invasion; (2) Patients with extrahepatic metastasis; (3) Patients who underwent noncurative liver resection; (4) Combined hepatocellular and cholangiocarcinoma diagnosed cases by histological findings; (5) History of allergy to contrast agents; (6) Patients with deranged kidney function or Child-Pugh C; (7) Pregnancy. The study population comprised 128 patients (101 men and 27 women) with a mean age of 52.7 years (range, 20–85 years). The patients underwent either laparotomy or laparoscopic operation. Hepatic surgery included anatomic resection and non-anatomic resection.

CT Image Acquisition
CT images of the liver obtained with a 64 slice multi-detector CT scanner (Optima CT660; GE Healthcare, Milwaukee, WI) by using the following parameters: gantry rotation times of 0.6 second for non-enhanced study and the hepatic arterial and portovenous phases, with 0.8 second for the equilibrium phase; a 5mm section thickness; 27.5mm/second table speed; 120kVp; and 160–440mA. Patients imaged with a CT scanner in a craniocaudal direction. The scan range is from the dome to the lower liver. Non-ionic contrast medium (Iohexol Injection) administered at a total dose of 70–80 mL according to body weight (0.9mL/kg) with an injection rate of 2.5–3.0 mL/second through a 20 gauge venous cannula placed in the antecubital vein. For triphasic acquisitions, scanning started with a 30 seconds scan delay (about 30–35 seconds after injection of the contrast

agent) for the hepatic arterial phase. Thirty-five seconds after the endpoint of the hepatic arterial phase (about 65–70 seconds after injection of the contrast agent), the scans for the portovenous phase acquired. Delayed phase images acquired 120 seconds (about 150–180 seconds after injection of the contrast agent).

MRI Image Acquisition

All MR images were acquired on a 3.0-T MR unit (Signa Excite; GE Medical Systems, Milwaukee, WI, USA) using an eight-channel, torso-phased-array coil centered over the liver. The MR images were obtained in the axial plane and with a rectangular field of view of 320–350 mm adjusted for the patient's body size. The baseline MR imaging was composed of the following sequences: respiratory-triggered, T2-weighted fast-spin echo (FSE); breath-hold, T2-weighted single-shot fast-spin echo (SSFSE); breath-hold, T1-weighted spoiled-gradient-recalled echo (GRE). Dynamic imaging, including the arterial phase, portal-venous phase (PVP), and delayed phase performed using the same fat-suppressed (FS), three-dimensional (3D), GRE sequence following administration of gadoxetic acid. All patients received a rapid bolus of a standard dose (0.025 mol/kg) of gadoxetic acid at a rate of 1.5 mL/ sec, immediately followed by a 30-mL saline flush through a catheter inserted into the antecubital vein. Imaging during the arterial phase was performed seven seconds after contrast agent arrival at the distal thoracic aorta, and subsequent PVP, delayed-phase imaging were performed at 50 seconds, 3 minutes respectively, after the administration of the contrast agent injection. Acquisition of FS-3D GRE data for each phase completed during a single breath-hold at the end of expiration (time range, 18–22 seconds; meantime, 19 seconds).

Histopathologic Examination

Resected specimens cut into 10-mm slices. Histopathologic examination revealed microscopic invasion as the presence of cancer cell clusters floating in the vascular space lined by endothelial cells. Tumor differentiation and histology of the noncancerous surrounding parenchyma defined according to the Liver Cancer Study Group of Japan guidelines.[28] Tumor grade defined by the poorest degree of differentiation.

Imaging Analysis

The imaging analysis performed on a dual-screen diagnostic workstation (GE Healthcare). The preoperative CT and MRI images were reviewed independently by two radiologists with 10 and 8 years of experience who blinded to the clinical information of each patient. On equilibrium phase, tumor margins were categorized into (Figure 1) smooth margin, presenting as a smooth tumor-normal liver interface; non-smooth margin, presenting as a focal outgrowth of nodules protruding into the non-tumor parenchyma; or non-smooth margin with multinodular type, presenting as multifocal outgrowths protruding into the nontumoral parenchyma.[11] We classified tumors preoperatively according to this classification using preoperative dynamic CT and MRI images.

Assessment of tumor capsules was in the equilibrium phase by identifying a thin, linear, enhanced structure encasing the tumor. According to the presence or absence of tumor capsules, tumors categorized into the following groups: capsules surrounding the tumor circumference, capsules that did not encompass the tumor circumference, or tumors without radiologic evidence of a tumor capsule.

Peritumoral enhancement defines as the existence of a detectable arterial-enhancing area adjacent to the tumor border on arterial phase images that became isodense or isointense compared with the liver parenchyma on equilibrium phase images.[29] The pattern of peritumoral
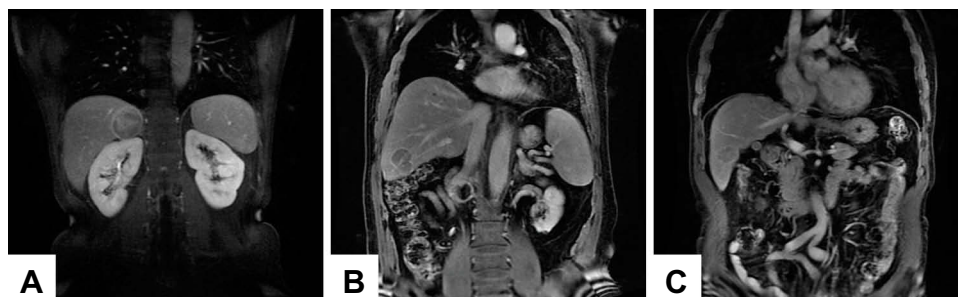

Figure 1 Contrast-enhanced MRI illustration of the patterns of tumor margin. Coronal view images: (**A**) Tumor with a smooth margin. (**B**) Tumor with focal extraocular extension. (**C**) Tumor with multinodular confluent appearance.

enhancement was categorized as absent or present (wedge-shaped or irregular circumferential enhancement) (Figure 2).

TTPVI was assessed and consisted of the identification of two separate features: the presence of internal arteries and hypoattenuating halos. An internal artery is the persistence of discrete arterial enhancement within the tumor assessed in the arterial phase, whereas hypodense halo is a rim of hypoattenuation partially or completely circumscribing the tumor evaluated in the portal venous or delayed phases[30] (Figure 3).

A third radiologist with 15 years of experience who was also blind to clinical information, resolved the differences between the two reviewers.

Statistical Analysis

The interobserver difference between the initial two observers evaluated with the Kappa test. Continuous data: tumor size between the positive and negative pMVI groups evaluated using an independent t-test. Categorical variables, such as sex, AFP, pathological tumor size, tumor differentiation, peritumoral enhancement, tumor margin, TTPVI, and tumor capsule, analyzed with the chi-square test or Fisher exact test. The parameters found to have statistical significance by univariate analysis were entered
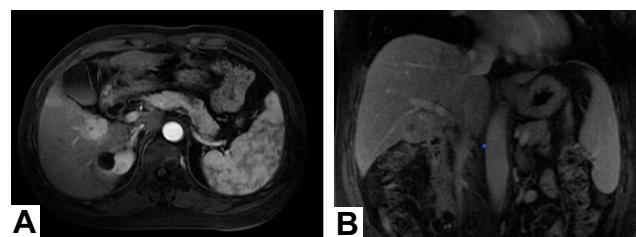

Figure 2 Contrast-enhanced MRI illustration of the peritumoral enhancement. (**A**) Axial view image showing detectable arterial-enhancing area adjacent to the tumor border on arterial phase images and (**B**) Coronal view images showing isointense signal compared with the liver parenchyma on equilibrium phase images.
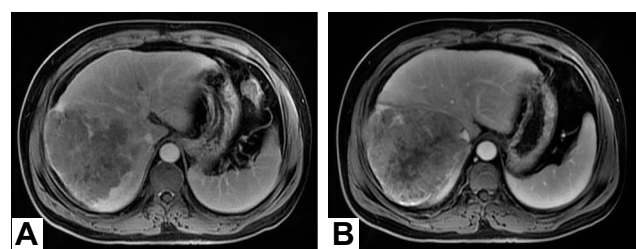

Figure 3 Contrast-enhanced MRI illustration of a two-trait predictor of venous invasion. Axial view images: (**A**) Tumor with the presence of internal arteries, and (**B**) Hypointense halos in the portal venous phase, suggestive of MVI.

into a multivariant logistic regression model to elucidate the independent predictors of pMVI. The odds ratio [OR] and confidence interval [CI] calculated for the parameters that showed statistical significance by multivariate logistic regression analysis. A p value <0.05 was considered to indicate a statistically significant difference. We calculated the diagnostic accuracy of the investigated radiologic features by measuring the positive and negative predictive values, as well as the area under the receiver operating characteristic curve. Finally, we have compared the difference between tumor size on CT and MRI and pathological tumor size with the Kappa test and the difference between subtypes of tumor margins on CT and MRI, respectively.

Results

A total of 128 preoperative patients, including 106 (82.8%) men and 22 (17.2%) women with HCC were enrolled in the study. The histopathological findings revealed that 61 HCC lesions were positive for pMVI, whereas 75 lesions were negative for pMVI. In our study, six patients had two lesions with pMVI, and two patients had two lesions without pMVI. There was an agreement between observers regarding the difference between tumor size on CT, MRI, and pathological tumor size (κ=0.71). The results of the univariate analysis of clinical characteristics and histopathological findings of patients with and without pMVI presented in (Table 1). Based on tumor size (microvascular invasion-positive group: 7.9±4.5cm; MVI-negative group: 3.6±2.7cm) showed statistically significant associations with pMVI. AFP level (p=0.043) collected and classified into two groups (<15ug/l, >15 ug/l), AFP level (>15 ug/l) was present in of 70% of HCCs (95 of 136). Tumor differentiation (Edmondson–Steiner grade), and pathological tumor size showed statistically significant associations with pMVI. Concerning sex, there was no statistically significant difference between the groups with and without pMVI.

Univariate analysis of radiological findings for patients with and without pMVI shown in (Table 2). Overall, nonsmooth tumor margins were present in 48.5% of HCCs (66 of 136 nodules). A focal multinodular margin was the most frequently diagnosed feature in 44.9% of nodules (61 of 136). TTPVI was present in 83% of nodules (113 of 136). We also compared the difference in tumor margins on CT and MRI. We found there was a significant difference between smooth and non-smooth margin on CT (p=0.043) and MRI (p<0.01) and subtypes of tumor margins on CT (p=0.047) and MRI (p=0.004) respectively.

Table 1 Univariate Analysis of Clinical Characteristics and Histopathological Findings of Patients with and Without Microvascular Invasion

Clinical Risk Factors	pMVI		p-value
	Negative (n=75)	Positive (n=61)	
Age, years (mean ±SD)	50±9.8	48±9.2	0.752
Sex			
Male	58	48	0.246
Female	15	7	
AFP level (ug/l)			
<15	28	13	0.043
≥15	47	48	
Size, cm (mean ± SD)	3.6±2.7	7.9±4.5	<0.01
Tumor differentiation (Edmondson-Steiner grade)			
G1-G2	45	17	<0.01
G3-G4	30	44	
Pathological tumor size (cm)			
≤3	40	7	<0.01
3~5	18	12	
5~10	13	25	
>10	4	17	

Table 2 Univariate Analysis of Radiological Findings for Patients with and Without Microvascular Invasion

rMVI	Total	pMVI		p-value
		Negative (n=75)	Positive (n=61)	
Tumor capsule				
Negative	32	19	13	0.714
Positive	104	56	48	
Incomplete capsule	75	39	36	
Complete capsule	29	17	12	
Peritumoral enhancement				
Negative	118	71	47	0.003
Positive	18	4	14	
Tumor margin				
Smooth	70	47	23	<0.01
Nonsmooth	66	28	38	
Focal extranodular	5	0	5	
Multinodular	61	28	33	
TTPVI				
Negative	23	20	3	<0.01
Positive	113	55	58	

Multivariate logistic regression analysis of risk factor in patients with and without pMVI is shown in (Table 3). Only tumor size, tumor differentiation and TTPVI had a statistically significant association with pMVI in both univariate and multivariate analysis. In multivariate logistic regression analysis, tumor size (odds ratio [OR] = 1.294; 95% confidence interval [CI]: 1.155, 1.451; $p < 0.001$), tumor differentiation (odds ratio [OR] =1.384; 95% confidence interval [CI]: 1.224, 1.564; $p < 0.001$), and TTPVI (odds ratio [OR] = 4.802; 95% confidence interval [CI]: 1.037, 22.233; $p=0.045$) were significant independent predictors of MVI. Using 5.8 as the threshold for size, one could obtain an area-under-curve (AUC) of 0.793 in ROC to differentiate between tumors with and without microvascular invasion, 95% Confidence interval [CI]: 0.715 to 0.857; $p < 0.001$, Sensitivity 64%, Specificity 88% (Figure 4), Positive predictive value (PPV) of TTPVI is 0.51, Negative predictive value (NPV) is 0.87.

Discussion

In our results, tumor size, tumor differentiation, TTPVI were the significant risk factors for pMVI of HCC in both

univariate and multivariate analyses. Two interobserver had a good agreement regarding it. We concluded that tumor size and histopathological differentiation were independent and significant predictors of pMVI in HCC. However, there are conflicting data regarding the usefulness of tumor size alone in predicting pMVI in HCC.[31] We also demonstrated that higher Edmondson-Steiner grades had a higher rate of pMVI. A similar study reported that tumor size, number, and Edmonson-Steiner grade were significant pre-operative predictors of pMVI,[32,33] which

Table 3 Multivariate Logistic Regression Analysis of Risk Factor in Patients with and Without Microvascular Invasion

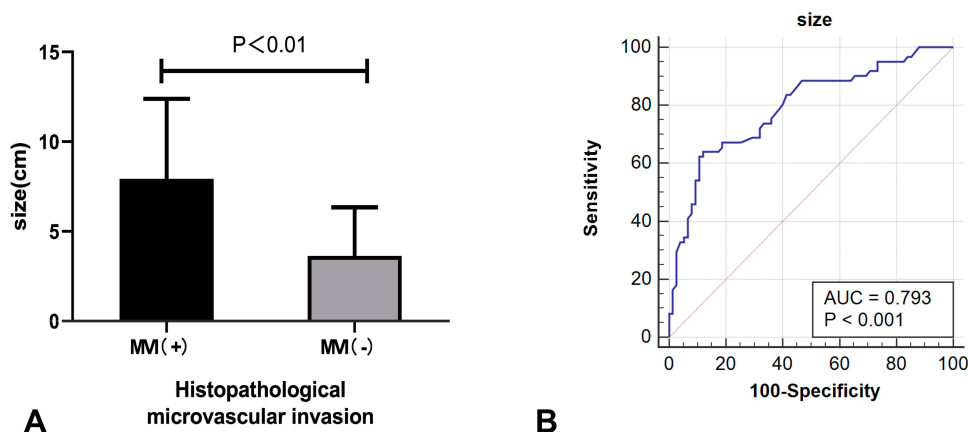| Risk Factor	Significance	Odds Ratio	95% Confidence Interval	
			Lower	Upper
Tumor size	<0.001	1.294	1.155	1.451
Tumor differentiation	<0.001	1.384	1.224	1.564
TTPVI	0.045	4.802	1.037	22.233

Figure 4 (A) The difference of tumor size between MVI positive and negative lesions. The tumor size shows a significant difference between the two groups. **(B)** ROC curve of size for predicting MVI.

is different from what was said by Sumie et al.[34] Previous reports on the relationship between tumor size and rate of pMVI demonstrated that large HCCs have a higher rate of VI.[35,36] Shirabe et al.[37] reported that the tumor size larger than 3.6cm as the predictors of pMVI. In a similar study, Kaibori et al.[32] reported the tumor size ≥5.0cm as the predictor. In our research, we concluded that the tumor size larger than 5.8cm as the predictors of pMVI.

Various studies have reported the gross pathological category as an essential predictor of portal vein invasion and intrahepatic metastasis in HCC.[38,39] Previous pathological studies have reported a higher risk of pMVI in single nodular with extraocular growth type and confluent multinodular type of HCC than the single nodular type.[34,40] However, we assessed the tumor margins only as either a smooth or a non-smooth margin, including focal extraocular and multinodular on dynamic CT and MRI images instead of following the gross pathological categories. In our result, tumor margin was significant for pMVI in univariate analysis, but it was not as a risk factor for pMVI. We also analyzed the difference between tumor margin on CT and MRI. We found a significant difference between smooth and non-smooth margin and subtypes of tumor margins of two groups of patients on CT and MRI, respectively, but it is not as an independent risk factor for pMVI. Differentiation between the confluent multinodular type and the single nodular type with extraocular growth by pre-operative CT imaging can be difficult, and we did not get imaging in the gadoxetic acid-enhanced HBP phase. The Calculation of the pathological gross size of the tumor showed that it was a significant risk factor of pMVI in univariate analysis. We have demonstrated the

difference between tumor size on CT, MRI was concordant with pathological tumor size.

The serum level of AFP is one of the most reliable diagnostic tumor markers for HCC. Eguchi et al.[39] reported that the AFP level could use as a predictor of latent pMVI and early recurrence. In our study, the serum AFP level showed a significant difference between negative and positive pMVI groups. However, multivariate logistic regression analysis is not a significant independent predictor of pMVI.

Peritumoral enhancement can reflect hemodynamic perfusion changes of HCC, which is useful for predicting MVI of HCC. Recently, several studies with gadoxetic acid-enhanced MRI have reported the peritumoral enhancement in the arterial phase as a parameter that is suggestive of an increased risk of pMVI.[30,41,42] However, Shan et al.[43] used radiomics to assess peritumoral enhancement delineated with a 2 cm expansion from the HCC; the AUC of peritumoral enhancement was up to 0.6. In our study, arterial peritumoral enhancement was not a significant independent factor for predicting pMVI. This might be the effect of the lower percentage of peritumoral enhancement in cases with HCC and a difference between different imaging modalities.

The relationship between tumor capsule, pMVI, and the post-operative recurrence remains unclear.[44,45] Several investigators have reported that radiologic evidence of tumor capsule correlated with pMVI and poor prognosis,[46] whereas other studies have demonstrated the presence of fibrous capsule as a favorable prognostic factor since the capsule might prevent the direct hepatic parenchymal invasion of HCC.[47] In our research, radiological tumor capsule and pMVI did not show a significant correlation, in good agreement with the results of previous studies.[11,18]

Segal et al.[25] have demonstrated TTPVI on CT are highly predictive for MVI. Renzulli et al.[30] showed a strong association of CT and MRI features with MVI and having the same diagnostic accuracy of both. They concluded the association between TTPVI, MVI, and the molecular profile might enable the use of imaging modalities to reconstruct the global gene expression programs of HCC in the future. Similarly, in our study, TTPVI was the only significant risk factor in rMVI for pMVI in both univariate and multivariate analyses. This might be due to the tumor being expansive, causing fibrosis and compression of liver tissue adjacent to the tumor margin, forming a hypoattenuating or hypointense halos. At the same time, tumor cells and their mesenchymal cells produce a large number of cytokines that promote angiogenesis, resulting in abundant neovascularization at the edge of the tumor, forming an intratumoral vascular sign.

However, the potential role of the new imaging techniques such as dual energy CT, function imaging of MRI, and further post-processing analysis such as texture analysis and radiomics has been reported to be useful findings for predicting pMVI. Hu et al.[48] have demonstrated the normalized iodine concentration (NIC) values of the three-phase scans have a specific positive correlation with microvessel density. Yang et al.[17] have shown iodine concentration (IC), NIC, and slope in the arterial phase (AP), and the ratio of IC difference between AP and venous phase (VP) has high diagnostic efficiency for pMVI. Function imaging findings, such as a lower apparent diffusion coefficient (Diffusion-Weighted Imaging),[18,49] mean kurtosis value (Diffusion kurtosis imaging),[20,50] and actual diffusion coefficient (Into-vexol Incoherent Movement)[21,51] have been reported the independent risk factor for pMVI of HCC. Texture analysis is a quantitative image processing algorithm that can use to quantify tissue heterogeneity by assessing the distribution of texture coarseness and irregularity within a lesion. Many studies have shown that texture analysis can not only predict pMVI but also predict early recurrence.[52,53] However, these criteria for preoperative imaging diagnosis of pMVI in HCC have not yet been widely recognized. Radiomics is a newly emerging form of imaging analysis using a series of datamining algorithms or statistical analysis tools on high-throughput imaging features to obtain predictive or prognostic information. Part of the study to date has assessed radiomics for pMVI in HCC patients.[23,24,54] Feng et al.[55] established a radiomics model predicting pMVI preoperatively by extracting radiomics features from the intratumoral and peritumoral regions of Gd-ethoxybenzyle-DTPA enhanced MRI, which is the first study to develop an MRI radiomics model

for pMVI prediction of HCC so far. Their results showed that the AUC, sensitivity, and specificity of the combined intratumoral and peritumoral radiomics model were 0.83, 90%, and 75%, respectively. Despite its potential, the use of radiomics as a clinical biomarker still necessitates amelioration and standardization.[56]

This study had some limitations. Since it was a retrospective study, we could not correlate tumor margin with pMVI. At the same time, the department of pathology of our hospital did not use the gross pathological category but categorized the tumor according to the size. Secondly, newer imaging methods, such as diffusion-weighted imaging, was not evaluated.

Conclusion

In conclusion, tumor size, tumor differentiation, TTPVI in preoperative CT, and MRI had a statistically significant association with MVI in both univariate and multivariate analyses. TTPVI may serve as an rMVI in predicting pMVI in cases and might play an important role in the future management of HCC by distinguishing MVI-positive patients during the decision-making stage for appropriate therapy. These results obtained by using CT and MRI imaging recommended for HCC diagnosis may potentially be useful for clinical practice.

Ethical Approval

This study was conducted in accordance with the declaration of Helsinki and Ethics Committee approved the study of Taihe Hospital, Shiyan, China (approval number: 2019KS010), and informed, written consent was obtained from all the subjects.

Disclosure

The authors have declared that no competing interests exist.

References

1. Torre LA, Bray F, Siegel RL, Ferlay J, Lortet-Tieulent J, Jemal A. Global cancer statistics, 2012. *CA Cancer J Clin*. 2015;65(2):87–108. doi:10.3322/caac.21262
2. Petitclerc L, Gilbert G, Nguyen BN, Tang A. Liver fibrosis quantification by magnetic resonance imaging. *Top Magn Reson Imaging*. 2017;26(6):229–241. doi:10.1097/RMR.0000000000000149
3. Takayama T, Makuuchi M, Hirohashi S, et al. Early hepatocellular carcinoma as an entity with a high rate of surgical cure. *Hepatology*. 1998;28(5):1241–1246. doi:10.1002/hep.510280511
4. Zhang BH, Yang BH, Tang ZY. Randomized controlled trial of screening for hepatocellular carcinoma. *J Cancer Res Clin Oncol*. 2004;130 (7):417–422. doi:10.1007/s00432-004-0552-0

5. Galati G, Dell'Unto C, Vespasiani-Gentilucci U, et al. Hepatocellular carcinoma in alcoholic liver disease: current management and recent advances. *Rev Recent Clin Trials*. 2016;11(3):238–252. doi:10.2174/1574887111999160701091605

6. Rodríguez-Perálvarez M, Luong TV, Andreana L, Meyer T, Dhillon AP, Burroughs AK. A systematic review of microvascular invasion in hepatocellular carcinoma: diagnostic and prognostic variability. *Ann Surg Oncol*. 2013;20(1):325–339. doi:10.1245/s10434-012-2513-1

7. Barreto SG, Brooke-Smith M, Dolan P, Wilson TG, Padbury RT, Chen JW. Cirrhosis and microvascular invasion predict outcomes in hepatocellular carcinoma. *ANZ J Surg*. 2013;83(5):331–335.

8. Portolani N, Coniglio A, Ghidoni S, et al. Early and late recurrence after liver resection for hepatocellular carcinoma: prognostic and therapeutic implications. *Ann Surg*. 2006;243(2):229–235. doi:10.1097/01.sla.0000197706.21803.a1

9. Iwatsuki S, Dvorchik I, Marsh JW, et al. Liver transplantation for hepatocellular carcinoma: a proposal of a prognostic scoring system. *J Am Coll Surg*. 2000;191(4):389–394. doi:10.1016/S1072-7515(00)00688-8

10. Shah SA, Cleary SP, Wei AC, et al. Recurrence after liver resection for hepatocellular carcinoma: risk factors, treatment, and outcomes. *Surgery*. 2007;141(3):330–339. doi:10.1016/j.surg.2006.06.028

11. Chou CT, Chen RC, Lin WC, Ko CJ, Chen CB, Chen YL. Prediction of microvascular invasion of hepatocellular carcinoma: preoperative CT and histopathologic correlation. *AJR Am J Roentgenol*. 2014;203(3):W253–259. doi:10.2214/AJR.13.10595

12. Bruix J, Sherman M. American association for the study of liver diseases, management of hepatocellular carcinoma: an update. *Hepatology*. 2011;53(3):1020–1022. doi:10.1002/hep.24199

13. Sumie S, Nakashima O, Okuda K, et al. The significance of classifying microvascular invasion in patients with hepatocellular carcinoma. *Ann Surg Oncol*. 2014;21(3):1002–1009. doi:10.1245/s10434-013-3376-9

14. Chen ZH, Zhang XP, Wang H, et al. Effect of microvascular invasion on the postoperative long-term prognosis of solitary small HCC: a systematic review and meta-analysis. *HPB*. 2019;21(8):935–944. doi:10.1016/j.hpb.2019.02.003

15. Lim KC, Chow PK, Allen JC, et al. Microvascular invasion is a better predictor of tumor recurrence and overall survival following surgical resection for hepatocellular carcinoma compared to the Milan criteria. *Ann Surg*. 2011;254(1):108–113. doi:10.1097/SLA.0b013e31821ad884

16. The general rules for the clinical and pathological study of primary liver cancer. liver cancer study group of japan. *Jpn J Surg*. 1989;19(1):98–129. doi:10.1007/BF02471576

17. Yang CB, Zhang S, Jia YJ, et al. Dual energy spectral CT imaging for the evaluation of small hepatocellular carcinoma microvascular invasion. *Eur J Radiol*. 2017;95:222–227. doi:10.1016/j.ejrad.2017.08.022

18. Xu P, Zeng M, Liu K, Shan Y, Xu C, Lin J. Microvascular invasion in small hepatocellular carcinoma: is it predictable with preoperative diffusion-weighted imaging? *J Gastroentero Hepatol*. 2014;29(2):330–336. doi:10.1111/jgh.12358

19. Huang M, Liao B, Xu P, et al. Prediction of microvascular invasion in hepatocellular carcinoma: preoperative Gd-EOB-DTPA-dynamic enhanced MRI and histopathological correlation. *Contrast Media Mol Imaging*. 2018;2018:9674565. doi:10.1155/2018/9674565

20. Cao L, Chen J, Duan T, et al. Diffusion kurtosis imaging (DKI) of hepatocellular carcinoma: correlation with microvascular invasion and histologic grade. *Quant Imaging Med Surg*. 2019;9(4):590–602. doi:10.21037/qims.2019.02.14

21. Wei Y, Huang Z, Tang H, et al. IVIM improves preoperative assessment of microvascular invasion in HCC. *Eur Radiol*. 2019;29(10):5403–5414. doi:10.1007/s00330-019-06088-w

22. Hyun SH, Eo JS, Song BI, et al. Preoperative prediction of microvascular invasion of hepatocellular carcinoma using 18F-FDG PET/CT: a multicenter retrospective cohort study. *Eur J Nucl Med Mol Imaging*. 2018;45(5):720–726. doi:10.1007/s00259-017-3880-4

23. Ni M, Zhou X, Lv Q, et al. Radiomics models for diagnosing microvascular invasion in hepatocellular carcinoma: which model is the best model. *Cancer Imaging*. 2019;19(1):60. doi:10.1186/s40644-019-0249-x

24. Xu X, Zhang HL, Liu QP, et al. Radiomic analysis of contrast-enhanced CT predicts microvascular invasion and outcome in hepatocellular carcinoma. *J Hepatol*. 2019;70(6):1133–1144. doi:10.1016/j.jhep.2019.02.023

25. Segal E, Sirlin CB, Ooi C, et al. Decoding global gene expression programs in liver cancer by noninvasive imaging. *Nat Biotechnol*. 2007;25(6):675–680. doi:10.1038/nbt1306

26. Lei Z, Li J, Wu D, et al. Nomogram for preoperative estimation of microvascular invasion risk in hepatitis B virus-related hepatocellular carcinoma within the milan criteria. *JAMA Surg*. 2016;151(4):356–363. doi:10.1001/jamasurg.2015.4257

27. Bruix J, Sherman M. Practice guidelines committee, american association for the study of liver diseases, management of hepatocellular carcinoma. *Hepatology*. 2005;42(5):1208–1236. doi:10.1002/hep.20933

28. Kudo M, Kitano M, Sakurai T, Nishida N. General rules for the clinical and pathological study of primary liver cancer, nationwide follow-up survey and clinical practice guidelines: the outstanding achievements of the liver cancer study group of Japan. *Dig Dis*. 2015;33(6):765–770. doi:10.1159/000439101

29. Kim H, Park MS, Choi JY, et al. Can microvessel invasion of hepatocellular carcinoma be predicted by pre-operative MRI. *Eur Radiol*. 2009;19(7):1744–1751. doi:10.1007/s00330-009-1331-8

30. Renzulli M, Brocchi S, Cucchetti A, et al. Can current preoperative imaging be used to detect microvascular invasion of hepatocellular carcinoma. *Radiology*. 2016;279(2):432–442. doi:10.1148/radiol.2015150998

31. Chandarana H, Robinson E, Hajdu CH, Drozhinin L, Babb JS, Taouli B. Microvascular invasion in hepatocellular carcinoma: is it predictable with pretransplant MRI. *AJR Am J Roentgenol*. 2011;196(5):1083–1089. doi:10.2214/AJR.10.4720

32. Kaibori M, Ishizaki M, Matsui K, Kwon AH. Predictors of microvascular invasion before hepatectomy for hepatocellular carcinoma. *J Surg Oncol*. 2010;102(5):462–468. doi:10.1002/jso.21631

33. Osório FM, Vidigal PV, Ferrari TC, Lima AS, Lauar GM, Couto CA. Histologic grade and mitotic index as predictors of microvascular invasion in hepatocellular carcinoma. *Exp Clin Transplant*. 2015;13(5):421–425. doi:10.6002/ect.2015.0045

34. Sumie S, Kuromatsu R, Okuda K, et al. Microvascular invasion in patients with hepatocellular carcinoma and its predictable clinicopathological factors. *Ann Surg Oncol*. 2008;15(5):1375–1382. doi:10.1245/s10434-008-9846-9

35. Kim SJ, Lee KK, Kim DG. Tumor size predicts the biological behavior and influence of operative modalities in hepatocellular carcinoma. *Hepatogastroenterology*. 2010;57(97):121–126.

36. Du M, Chen L, Zhao J, et al. Microvascular invasion (MVI) is a poorer prognostic predictor for small hepatocellular carcinoma. *BMC Cancer*. 2014;14:38. doi:10.1186/1471-2407-14-38

37. Shirabe K, Toshima T, Kimura K, et al. New scoring system for prediction of microvascular invasion in patients with hepatocellular carcinoma. *Liver Int*. 2014;34(6):937–941. doi:10.1111/liv.12459

38. Nagano Y, Shimada H, Takeda K, et al. Predictive factors of microvascular invasion in patients with hepatocellular carcinoma larger than 5 cm. *World J Surg*. 2008;32(10):2218–2222. doi:10.1007/s00268-008-9585-x

39. Eguchi S, Takatsuki M, Hidaka M, et al. Predictor for histological microvascular invasion of hepatocellular carcinoma: a lesson from 229 consecutive cases of curative liver resection. *World J Surg*. 2010;34(5):1034–1038. doi:10.1007/s00268-010-0424-5

40. Shimada M, Rikimaru T, Hamatsu T, et al. The role of macroscopic classification in nodular-type hepatocellular carcinoma. *Am J Surg*. 2001;182(2):177–182. doi:10.1016/S0002-9610(01)00682-1

41. Ahn SY, Lee JM, Joo I, et al. Prediction of microvascular invasion of hepatocellular carcinoma using gadoxetic acid-enhanced MR and (18) F-FDG PET/CT. *Abdom Imaging*. 2015;40(4):843–851. doi:10.1007/s00261-014-0256-0

42. Ünal E, İdilman İS, Akata D, Özmen MN, Karçaaltıncaba M. Microvascular invasion in hepatocellular carcinoma. *Diagn Interv Radiol*. 2016;22(2):125–132. doi:10.5152/dir.2015.15125

43. Shan QY, Hu HT, Feng ST, et al. CT-based peritumoral radiomics signatures to predict early recurrence in hepatocellular carcinoma after curative tumor resection or ablation. *Cancer Imaging*. 2019;19 (1):11. doi:10.1186/s40644-019-0197-5

44. Shirabe K, Kanematsu T, Matsumata T, Adachi E, Akazawa K, Sugimachi K. Factors linked to early recurrence of small hepatocellular carcinoma after hepatectomy: univariate and multivariate analyses. *Hepatology*. 1991;14(5):802–805. doi:10.1002/hep.1840140510

45. Nagasue N, Uchida M, Makino Y, et al. Incidence and factors associated with intrahepatic recurrence following resection of hepatocellular carcinoma. *Gastroenterology*. 1993;105(2):488–494. doi:10.1016/0016-5085(93)90724-Q

46. Witjes CD, Willemssen FE, Verheij J, et al. Histological differentiation grade and microvascular invasion of hepatocellular carcinoma predicted by dynamic contrast-enhanced MRI. *J Magn Reson Imaging*. 2012;36(3):641–647. doi:10.1002/jmri.23681

47. Ng IO, Lai EC, Ng MM, Fan ST. Tumor encapsulation in hepatocellular carcinoma. A pathologic study of 189 cases. *Cancer*. 1992;70 (1):45–49. doi:10.1002/1097-0142(19920701)70:1<45::AID-CNCR2820700108>3.0.CO;2-7

48. Hu S, Huang W, Chen Y, et al. Spectral CT evaluation of interstitial brachytherapy in pancreatic carcinoma xenografts: preliminary animal experience. *Eur Radiol*. 2014;24(9):2167–2173. doi:10.1007/s00330-014-3257-z

49. Zhao J, Li X, Zhang K, et al. Prediction of microvascular invasion of hepatocellular carcinoma with preoperative diffusion-weighted imaging: A comparison of mean and minimum apparent diffusion coefficient values. *Medicine*. 2017;96(33):e7754. doi:10.1097/MD.0000000000007754

50. Wang WT, Yang L, Yang ZX, et al. Assessment of microvascular invasion of hepatocellular carcinoma with diffusion kurtosis imaging. *Radiology*. 2018;286(2):571–580. doi:10.1148/radiol.2017170515

51. Zhao W, Liu W, Liu H, et al. Preoperative prediction of microvascular invasion of hepatocellular carcinoma with IVIM diffusion-weighted MR imaging and Gd-EOB-DTPA-enhanced MR imaging. *PLoS One*. 2018;13(5):e0197488. doi:10.1371/journal.pone.0197488

52. Ahn SJ, Kim JH, Park SJ, Kim ST, Han JK. Hepatocellular carcinoma: preoperative gadoxetic acid-enhanced MR imaging can predict early recurrence after curative resection using image features and texture analysis. *Abdom Radiol*. 2019;44(2):539–548. doi:10.1007/s00261-018-1768-9

53. Zhu YJ, Feng B, Wang S, et al. Model-based three-dimensional texture analysis of contrast-enhanced magnetic resonance imaging as a potential tool for preoperative prediction of microvascular invasion in hepatocellular carcinoma. *Oncol Lett*. 2019;18(1):720–732. doi:10.3892/ol.2019.10378

54. Peng J, Zhang J, Zhang Q, Xu Y, Zhou J, Liu L. A radiomics nomogram for preoperative prediction of microvascular invasion risk in hepatitis B virus-related hepatocellular carcinoma. *Diagn Interv Radiol*. 2018;24(3):121–127. doi:10.5152/dir.2018.17467

55. Feng ST, Jia Y, Liao B, et al. Preoperative prediction of microvascular invasion in hepatocellular cancer: a radiomics model using Gd-EOB-DTPA-enhanced MRI. *Eur Radiol*. 2019;29(9):4648–4659. doi:10.1007/s00330-018-5935-8

56. Limkin EJ, Sun R, Dercle L, et al. Promises and challenges for the implementation of computational medical imaging (radiomics) in oncology. *Ann Oncol*. 2017;28(6):1191–1206. doi:10.1093/annonc/mdx034